Cerebral Cortex, July 2018;28: 2525–2539

doi: 10.1093/cercor/bhy062
Advance Access Publication Date: 18 April 2018
Original Article

ORIGINAL ARTICLE

Neurocognitive Profiles of Older Adults with Working-Memory Dysfunction

Alireza Salami [1,2], Anna Rieckmann[2,3], Nina Karalija[2,3], Bárbara Avelar-Pereira[1,2], Micael Andersson[3,4], Anders Wåhlin[2], Goran Papenberg[1], Douglas D. Garrett[5], Katrine Riklund[2,3], Martin Lövdén[1], Ulman Lindenberger[5], Lars Bäckman[1] and Lars Nyberg[2,3,4]

[1]Aging Research Center, Karolinska Institutet and Stockholm University, S-11330 Stockholm, Sweden, [2]Umeå Center for Functional Brain Imaging (UFBI), Umeå University, S-90187 Umeå, Sweden, [3]Department of Radiation Sciences, Umeå University, S-90187 Umeå, Sweden, [4]Department of Integrative Medical Biology, Umeå University, S-90187 Umeå, Sweden and [5]Center for Lifespan Psychology, Max Planck Institute for Human Development, D-14195 Berlin, Germany

Address correspondence to Alireza Salami, Aging Research Center, Karolinska Institutet, Gävlegatan 16, S-113 30 Stockholm, Sweden. Email: alireza.salami@ki.se orcid.org/0000-0002-4675-8437

Alireza Salami and Anna Rieckmann have equally contributed to this work

Abstract

Individuals differ in how they perceive, remember, and think. There is evidence for the existence of distinct subgroups that differ in cognitive performance within the older population. However, it is less clear how individual differences in cognition in old age are linked to differences in brain-based measures. We used latent-profile analysis on n-back working-memory (WM) performance to identify subgroups in a large sample of older adults (n = 181; age = 64–68 years). Our analysis identified one larger normal subgroup with higher performance (n = 113; 63%), and a second smaller subgroup (n = 55; 31%) with lower performance. The low-performing subgroup showed weaker load-dependent BOLD modulation and lower connectivity within the fronto-parietal network (FPN) as well as between FPN and striatum during n-back, along with lower FPN connectivity at rest. This group also exhibited lower FPN structural integrity, lower frontal dopamine D2 binding potential, inferior performance on offline WM tests, and a trend-level genetic predisposition for lower dopamine-system efficiency. By contrast, this group exhibited relatively intact episodic memory and associated brain measures (i.e., hippocampal volume, structural, and functional connectivity within the default-mode network). Collectively, these data provide converging evidence for the existence of a group of older adults with impaired WM functioning characterized by reduced cortico-striatal coupling and aberrant cortico-cortical integrity within FPN.

Key words: dopamine, fronto-parietal network, functional connectivity, individual differences, working memory

Introduction

Cognitive impairment in aging may come in several different forms (Buckner 2004). One type of impairment is characterized by atrophy in the medial-temporal lobe (MTL) and posterior cortical regions, which often ensures deficits on long-term memory tasks (Nyberg and Bäckman 2010; Gorbach et al. 2016) and may predict Alzheimer's disease (AD) (Devanand et al. 2007; Kantarci et al. 2016; Mak et al. 2016). A second type is associated with larger age-related alterations in the fronto-parietal cortex and subcortical regions, and is related to impaired performance on working memory (WM) and various executive tasks (West 1996; Dahlin et al. 2008; Salami et al. 2013; Di et al. 2014). In addition, large-scale population-based studies have demonstrated substantial inter-individual differences in cognitive performance across the human lifespan (Lindenberger 2014), with a sizable proportion of older adults showing little to no impairment in memory or executive functioning (Glisky et al. 2001; Josefsson et al. 2012; Nyberg et al. 2012). Thus, there is converging evidence from several lines of research for the existence of distinct cognitive subgroups within the older population.

Despite the fact that WM has been much studied in the context of aging, brain-related factors linked to well-preserved WM in old age remain insufficiently characterized, likely reflecting a lack of comprehensive assessment of brain integrity, measured by different in vivo imaging modalities as well as genetic measures. Specifically, there is no study to date that simultaneously integrates neurochemical, structural, functional and genetic measures to identify brain-related factors of well-preserved WM functioning in aging. Another issue that has not been addressed in previous work concerns identification and characterization of potential WM subgroups. Most previous studies have reported a linear association between age-related changes in brain and behavior (Cabeza et al. 2016). However, such associations may also be non-linear and only detectable in certain subgroups, when a certain threshold of brain deterioration has been reached (Burzynska et al. 2012). Therefore, we used latent-profile analysis (LPA) which is a Gaussian mixture-modeling approach for identifying hidden population subgroups (Vermunt and Magidson 2002). Each individual has a probability of belonging to a certain subgroup, which allows for characterizing subgroups on other variables without assuming absolute group membership, thus boosting classification accuracy. LPA has been shown to capture population heterogeneity by identifying clinically relevant subgroups in different neurological disorders such as AD (Scheltens et al. 2016), Parkinson's disease (Flensborg Damholdt et al. 2012), but also among normal elderly adults (Ko et al. 2007; Pruchno et al. 2010; Hayden et al. 2011; Fandako et al. 2012; Lövden et al. 2017), and has the advantage of being purely data-driven and independent of a pre-determined cut-offs such as the median. We applied LPA on WM performance data from in-scanner and a number of offline tests to identify subgroups in a large age-homogenous sample of older adults (n = 180; 64–68 years). Using this multivariate data-driven approach, we expected to observe a minimum of two subgroups, likely reflecting normal versus low-performing older individuals with regard to WM functioning.

In the next step, the identified subgroups were compared on a rich set of demographics, health, genetic, and structural and functional brain imaging variables to explore whether latent profiling of older adults on a single cognitive task can capture differences in neurobiological integrity for some of the examined variables. For this, we first examined group differences in functional brain responses (amplitude and connectivity) within the canonical fronto-parietal network (FPN), but also within the dorsal attention network (DAN) and default mode network (DMN) during n-back performance, as well as during resting-state. Individual differences in WM have been linked to individual differences in blood-oxygen-level dependent (BOLD) signal responsivity within the DMN (Liang et al. 2016) and the FPN (Nagel et al. 2009; Spencer-Smith et al. 2013; Darki and Klingberg 2015; Huang et al. 2016), but not within the DAN (Grady et al. 2016). Specifically, BOLD signal in the FPN has been shown to be less responsive to increasing WM demands in low-performing older subgroups (Nagel et al. 2009; Nyberg et al. 2009). Relatedly, individual differences in load-dependent functional connectivity have been shown to predict individual differences in WM performance (Nagel et al. 2011; Newton et al. 2011; Huang et al. 2016). Moreover, there is evidence for age differences in functional connectivity at rest, including differences in the FPN (Salami et al. 2014; Grady et al. 2016; Jockwitz et al. 2017), suggesting that subgroups may also differ in resting-state connectivity.

Next, we examined group differences in structural MRI data, resting cerebral blood flow, and dopamine (DA)-system integrity. Older individuals with lower WM performance show reduced global white matter integrity (Vernooij et al. 2009), particularly within frontal pathways (Davis et al. 2009; Burzynska et al. 2011), as well as accelerated atrophy in prefrontal (Raz et al. 1997; Gunning-Dixon and Raz 2003; Yuan and Raz 2014), but also parietal and subcortical (Manard et al. 2016) regions. In addition, resting cerebral blood flow in prefrontal regions increases in response to WM training (Takeuchi et al. 2013). Therefore, we examined if older individuals with lower WM performance exhibit lower FP cerebral blood and increased coupling between resting cerebral blood flow and WM.

DA receptor availability decreases with age (Volkow et al. 1996; Rieckmann et al. 2011) and has been linked to age-related cognitive deficits (Bäckman et al. 2010). However, the role of DA D2 receptors in WM has not been firmly established (Cools and D'Esposito 2011), but some studies suggest that D_2 receptors are implicated in striatal-based updating of WM contents (Frank et al. 2001; Mehta et al. 2004; Bäckman et al. 2011; D'Esposito and Postle 2015). Relatedly, animal studies show that frontal DA D_2 receptors impact attention and flexibility aspects of WM (Floresco et al. 2006; Puig and Miller 2015; Ott and Nieder 2016). Computational models also suggest that DA D2 activity might put prefrontal networks in a more flexible state and enhance WM coding (Ott and Nieder 2016). Thus, it is reasonable to expect that older individuals with lower WM performance and lower functional and structural brain integrity are also characterized by reduced DA D_2 receptor availability, possibly within the frontal region. Such a finding would not only inform our understanding of WM in aging but also provide novel evidence for the role of (prefrontal) D2 receptors in WM. That said, in order not to limit our investigation to one aspect of the DA system, we also take a genomic imaging approach to study the relationship between the DA and WM.

Between-person variability in WM performance has previously been linked, in part, to DA gene variants (Barnes et al. 2011; Nikolova et al. 2011), such as the Catechol-O-Methyltransferase (COMT) Val^{158}Met polymorphism (Nagel et al. 2008), and allelic variants have been associated with differences in task-associated functional brain responses (Nyberg et al. 2013; Papenberg et al. 2015). Single-nucleotide polymorphisms (SNPs) located in the D2-receptor gene and in proteins relevant to DA-signaling pathways are other examples of genes associated with WM performance, as well as with brain structure and function and neurochemistry

(Hirvonen et al. 2009; Colzato et al. 2016). Given that brain responses and behavior are controlled by a wide variety of genes (Li et al. 2013), we compared group differences for the presence of allelic variants of SNPs that have been associated with differences in striatal and frontal DA levels.

Finally, we compared groups on selected demographic and health-related variables, as prior evidence supports a link between WM functioning and demographic (e.g., education) and vascular factors (Boone 1999; Plumet et al. 2005).

Materials and Methods

A detailed description of the recruitment procedure, imaging protocols, and cognitive and life-style assessments in the Cognition, Brain, and Aging (COBRA) study have been published (Nevalainen et al. 2015; Nyberg et al. 2016; Lövden et al. 2017). Here, we describe the methods directly relevant to the present study.

Participants

The sample consisted of 180 older individuals (64–68 years; mean = 66.2, SD = 1.2; 81 women) randomly selected from the population register of Umeå, in northern Sweden. Exclusion criteria included suspected brain pathology, impaired cognitive functioning (Mini Mental State Examination <27), and conditions that could bias the measurements of brain (e.g., severe trauma, tumors), cognitive performance (e.g., severely reduced vision) or preclude imaging (e.g., metal implants). 28% of the sample was working, 18% used nicotine, and 33% took blood-pressure medications. Mean education was 13.3 years (SD = 3.5), body-mass index (BMI) was 26.1 (SD = 3.5), systolic blood pressure was 142 (SD = 17), and diastolic blood pressure was 85 (SD = 10). The sample is representative of the healthy target population in Umeå (Nevalainen et al. 2015).

In-scanner Task

Performance data (sum of correct responses) were obtained from a numerical *n*-back task. In this task, a sequence of single numbers appeared on the screen. Each number was shown for 1.5 s, with an ISI of 0.5 s. During every item presentation, participants reported if the number currently seen on the screen was the same as that shown 1, 2, or 3 digits back. A heading that preceded each subtest indicated the actual condition. Participants responded by pressing one of two adjacent buttons with the index or middle finger to reply "yes, it is the same number" or "no, it is not the same number", respectively. A single fMRI run with 9 blocks for each condition (1-, 2-, and 3-back) was performed in random order (inter-block interval: 22 s), each block consisting of 10 items for each subject of which 4 were targets. The trial sequence was the same for all participants with only two lures (a single 2-back lure within two of the 3-back blocks). The n-back blocks were counterbalanced. The mean starting time for the different conditions was 313 s, 306 s, and 296 s, respectively.

Offline Cognitive Measures

The main cognitive domains examined offline in COBRA are WM, episodic memory, and perceptual speed (Nevalainen et al., 2015). These domains were tested with 3 separate tasks each (a verbal, a numerical, and a figural task). For each task, summary scores were computed across the total number of blocks or trials. Task summary scores were standardized (T-score: Mean = 50; SD = 10), to form a composite for each task and averaged across cognitive domain to generate domain-specific summary scores.

Working Memory

Letter-Updating Task

A sequence of letters (A–D) appeared one-by-one on the computer screen, and participants were instructed to continuously update and remember the 3 lastly shown letters. Letters were presented during 1 s, with an ISI of 0.5 s. Then, at an unknown time point in the sequence, the 3 last letters were to be typed in using the keyboard. In case of failure, participants guessed. The test consisted of 16 trials, with 4 trials of 7, 9, 11, or 13 letter sequences presented in random order.

Columnized Numerical 3-Back Task

A grid consisting of 1 × 3 boxes was presented on the screen. In each box, one at a time and starting from the left, a number (1–9) was presented for 1.5 s, with the next number presented after an ISI of 0.5 s. After a number was presented in the rightmost box, the next number appeared in the leftmost box. In each trial, 30 numbers were presented. The task consisted of deciding whether the number appearing in a specific box was the same as the last number displayed in that particular box. A response was required for all 3 boxes throughout the test, by pressing labeled keys on the keyboard that corresponded to "yes" (right index finger) or "no" (left index finger). The first 3 numbers all received a "no", as no numbers had appeared before that.

Spatial-Updating Task

Participants were presented with 3 separate grids (3 × 3 squares in each) that were placed adjacent to each other. Three circular objects, one at a random position in each grid, were presented simultaneously for 4 s, after which they disappeared. Following this, an arrow appeared beneath each grid for 2.5 s (one at a time, from left to right, with an ISI of 0.5 s), pointing in the direction where each circle should be mentally moved. This manipulation was done twice for each grid (i.e., 6 updating operations in total). Following updating, participants were asked to mark the correct object position in each grid, using the computer mouse. In case of uncertainty, participants guessed the position of the object. The test consisted of 10 test trials.

Perceptual Speed

Letter-Comparison Task

Two 4-letter strings were shown adjacent, but separated, from each other. The task consisted of deciding whether the pairs of items, built up by letters a–z, were identical or differed in the sequence code. For different letter strings, only one letter differed. During item presentation, participants responded by pressing designated buttons. When participants had responded, the sequence disappeared. The same event took place if no response was given within 5 s (timeout). The ISI between a response or timeout and appearance of a new item was 0.5 s. Each trial consisted of 40 item pairs, of which half were identical and intermixed with the other half of differing pairs. Scores were calculated by dividing the number of correct responses by the total response time (i.e., for both correct and incorrect responses; in milliseconds) and multiplying this quotient by 60 000 (i.e., creating a score of correct responses per minute, which penalizes incorrect responses).

Number-Comparison Task

The design of this task was similar to that of the letter-comparison task, the only difference being that the items contained 4-number strings (comprised of numbers 1–9) instead of letters.

Figure-Comparison Task

The procedures were similar to the other comparison tasks, except that participants were presented with two figures ("fribbles"; courtesy of Michael J. Tarr, Brown University, Providence, RI, USA, http://www.tarrlab.org) that were adjacently positioned, with some space in between, on the display. For the different figures, one constituent of the figures was different.

Episodic Memory

Word Recall

Participants were presented with 16 Swedish words (nouns) that appeared consecutively on the screen. The words were concrete, easy to spell, and all differed in the first 3 letters. During encoding, words were presented for 6 s each, with an ISI of 1 s. After having seen the entire list of 16 items, participants reported the words they could recall by writing them one-by-one in any order. Two test trials were administered (max = 32).

Number-Word Task

This task consisted of memorizing pairs of 2-digit numbers and concrete plural nouns (e.g., 46 dogs). During encoding, 8 number-word pairs were displayed for 6 s each, with an ISI of 1 s. Following encoding, participants were requested to report, using the keyboard, the 2-digit number that was associated with each noun shown on the screen. (e.g., How many dogs?) Upon reporting, words were presented one-by-one in a different order than during acquisition. Two test trials were administered.

Object-Position Memory Task

Participants were presented with a grid of 6 × 6 squares. One at a time, 12 objects were shown, each at separate locations in the grid. Presentation time of each object-position pair was 8 s, with an ISI of 1 s. At retrieval, all objects were shown adjacent to the grid and the correct position of each object was reported by moving objects with the computer mouse (in any order) to the correct location in the grid. If failing to recall the position, participants guessed. Two test trials were performed.

Verbal Knowledge

Participants performed a vocabulary test (Dureman, 1960). Thirty words were presented and for each target word, a correct synonym out of 5 possible alternatives was to be selected. The maximum score for this task was 30 (one credit score for each correct synonym).

Behavioral Profiling

Rather than relying on an arbitrary a-priori cut-off, such as the median, LPA is a data-driven method that can operate on multiple indicator variables (1-back, 2-back, and 3-back) to identify latent WM subgroups in the n-back data by entering summary scores from each condition as separate variables. For supplementary information, an alternative model was based on summary scores from the 3 WM offline tests. Overlap between classifications was computed to estimate to what degree in-scanner profiling generalizes to offline WM data. Individuals that were classified as normal performing based on in-scanner data but were low-performing on offline data, and vice versa, were excluded from supplementary analysis because of low confidence in their group allocation. LPA was implemented with Gaussian-mixture modeling. The Bayesian information criterion (BIC) and bootstrap likelihood ratio test (LRT) were used to compare models with the number of classes varying from 1 to 5. The model with the lowest BIC was selected as the optimal description of latent classes in the data. The analyses were implemented in R's Mclust package (http://cran.r-project.org/web/packages/mclust/index.html)

In order to characterize the subgroups further in terms of their behavioral profile, they were compared on offline domain summary scores with a domain × group ANOVA and follow-up independent *t*-tests on domain summary scores and individual tests. To elucidate possible inter-relations among domain group differences, a multiple regression analysis was included with offline WM summary score as the dependent variable and group, offline summary scores for episodic memory, speed, and SRB as predictors. An absence of a group effect would indicate that WM group differences are explained by group differences in any of the other predictors.

Image Acquisition

Magnetic resonance (MR) imaging was performed with a 3 Tesla Discovery MR 750 scanner (General Electric, WI, US), equipped with a 32-channel phased-array head coil. Positron Emission Tomography (PET) was done with a Discovery PET/CT 690 scanner (General Electric, WI, USA).

Structural MR Imaging

A 3D fast-spoiled echo sequence was used for acquiring anatomical T1-weighted images, collected as 176 slices with a thickness of 1 mm. TR = 8.2 ms, flip angle = 12 degrees, and field of view = 25 × 25 cm.

Cerebral Blood Flow

Whole-brain cerebral-blood flow was measured with 3D pseudo-continuous arterial spin labeling (ASL). Labeling time was 1.5 s, post-labeling delay time was 1.5 s, field of view was 24 cm, slice thickness was 4 mm, number of averages was 3, number of control label pairs was 30, and acquisition resolution was 8 × 512 (arms × data points in spiral scheme). Cerebral blood flow (CBF) maps were computed yielding tissue CBF in mL/min/100 g.

Functional MR Imaging

BOLD-contrast sensitive scans were acquired using a T2*-weighted single-shot gradient echoplanar-imaging sequence. Parameters were: 37 transaxial slices, 3.4 mm thickness, 0.5 mm spacing, TE/TR = 30/2000 ms, 80 degrees flip angle, 25 × 25 cm field of view, and a 96 × 96 acquisition matrix (Y direction phase encoding). At the start, 10 dummy scans were collected. The functional data were acquired during resting-state conditions (6 min) followed by the numerical n-back WM task described above.

Diffusion-Weighted Imaging

White-matter integrity was examined with diffusion-tensor imaging (DTI). These images were acquired by a spin-echo-planar T2-weighted sequence, using 3 repetitions and 32 independent directions. The total slice number was 64, with a TR of 8000 ms, a TE of 84.4 ms, a flip angle of 90 degrees, a field of view of 25 × 25 cm, and with $b = 1000$ s/mm^2 (Y direction phase encoding). The data matrix was interpolated to a 256 × 256 matrix with an up-sampled spatial resolution of 0.98 × 0.98 × 2 mm.

PET Image Acquisition

PET was performed during resting-state conditions following an intravenous bolus injection of 250 MBq ^{11}C-raclopride. Preceding the injection, a 5 min low-dose helical CT scan (20 mA, 120 kV, 0.8 s/revolution) was obtained, for the purpose of attenuation correction. Following the bolus injection, a 55-min 18-frame dynamic scan was acquired. Attenuation- and decay-corrected images (47 slices, field of view = 25 cm, 256 × 256-pixel transaxial images, voxel size = 0.977 × 0.977 × 3.27 mm) were reconstructed with filter-back-projection (FBP), using 6 iterations, 24 subsets, and 3.0 mm post filtering, yielding full width at half maximum (FWHM) of 3.2 mm (Wallsten et al. 2013). Head movements during the imaging session were minimized with an individually fitted thermoplastic mask attached to the bed surface. From the initial sample (n = 180), 12 subjects misunderstood fMRI n-back task (see subgroup 3 in the Results section), 6 subjects lacked DA data, 3 were statistical outliers, and 13 had missing FBP data. Thus, data from 146 subjects (n (normal-performing) = 95; n (low-performing) = 51) were included in this analysis. For 82% of the individuals, PET was carried out 2 days after the MR-scan (average time difference between MRI and PET: 3 ± 6 days).

Image Processing

PET Images

The following preprocessing steps were performed for each subject in SPM8. The 18 frame PET scans were coregistered to the T1-image using the time-frame-mean of the PET images as source. They were then normalized to MNI-space with the subject-specific flow fields (obtained with DARTEL) and then were affine transformed, and smoothed via a Gaussian filter of 8 mm. Normalization parameters were selected so that concentrations in the images were preserved. For determination of D2DR BP, time–activity curves for each voxel were entered into a Logan analyses (Logan et al. 1990), using time–activity curves in the gray-matter parts of cerebellum as reference.

Volumetric MRI Processing

To quantify gray-matter volumes, T1-weighted images were first segmented into gray matter, white matter, and cerebrospinal fluid, using the unified segmentation approach (Ashburner and Friston 2005) in SPM [Statistical Parametric Mapping, Wellcome Trust Centre for Neuroimaging, http://www.fil.ion.ucl.ac.uk/spm/] implemented in Matlab 10 (The Mathworks, Inc). The "light clean up" option was used to remove odd voxels from the segments. The gray-matter images were further analyzed using DARTEL (Ashburner 2007) in SPM. The gray-matter segments were imported into DARTEL space, and a final customized template was created, as were subject-specific flow fields containing the individual spatial-normalization parameters (diffeomorphic non-linear image registration). These segments were further warped into standard MNI space, by incorporating an affine transformation mapped from the DARTEL template to MNI space. In addition, the normalized gray-matter volumes were modulated by scaling these with Jacobian determinants from the registration step to preserve local-tissue volumes. Volumes were smoothed with an FWHM Gaussian kernel of 8 mm in the 3 directions. Here, we ran a two-sample t-test to compare gray-matter volume within the canonical FPN as well as total gray-matter volume between subgroups.

Diffusion-Weighted Image Processing

Diffusion-weighted data analysis was performed using the University of Oxford's Center for Functional Magnetic Resonance Imaging of the Brain (FMRIB) Software Library (FSL) package (http://www.fmrib.ox.ac.uk/fsl) and tract-based spatial statistics (TBSS), as part of the FMRIB software package. The full details of DTI data analyses (using identical imaging parameters but on a different sample) were given elsewhere (Salami et al. 2011). In short, the 3 subject-specific diffusion acquisitions were concatenated in time and corrected for eddy correct-induced distortions and head motion. Accordingly, the b-matrix was reoriented based on the transformation matrix (Leemans and Jones 2009). Next, the first volume within the averaged volume that did not have a gradient applied (i.e., the first b = 0) was used to generate a binary brain mask with the Brain Extraction Tool (Smith 2002). Finally, DTIfit was used to fit a diffusion tensor to each voxel included in the brain mask. As such, voxel-wise maps of fractional anisotropy (FA) were obtained. Using the TBSS processing stream, all subject-specific FA maps were nonlinearly normalized to standard space (FMRIB58_FA) and then fed into a skeletonize program to make a skeleton of common white-matter tracts across all subjects. Averaged FA along the spatial course of 11 major tracts (Salami et al. 2011) were computed with reference to the JHU ICBM-DTI-81 white-matter labels, distributed in the FSL package (Wakana et al. 2004). There were 2 subjects (one from each group) with missing DTI data (n (normal-performing) = 112; n (low-performing) = 54).

Functional MRI Analyses

Preprocessing of the fMRI data included slice-timing correction and motion correction by unwarping and realignment to the first image of each volume. The realignment routine calculates 3 translation parameters (x, y, and z) and 3 rotation parameters (roll, pitch, and jaw) reflecting the location of each volume compared to the first volume. The fMRI volumes were normalized to a sample-specific template, using DARTEL (Ashburner 2007), affine alignment to MNI standard space, and spatial smoothing with an 8-mm FWHM Gaussian kernel. As a first order analysis, a general linear model with regressors for each load condition (1-back, 2-back, 3-back), convolved with a hemodynamic response function, and the 6 realignment parameters from the movement correction as covariates of no interest, was set up. Each block was 20 s and there were 9 blocks per n-back-condition. Three fixation periods of 20 s each formed an implicit baseline. A-priori ROI analyses were chosen for primary analyses in order to avoid sample-specific bias (e.g., toward the larger group or toward task-based vs. resting-state BOLD).

ROIs were selected based on existing literature (Vincent et al. 2008) to capture key nodes of 3 large-scale association networks (Supplementary Table 1): The canonical WM fronto-parietal network (FPN: bilateral anterior and dorsolateral PFC, anterior cingulate, bilateral insula, and bilateral anterior inferior parietal lobe), the default mode network (DMN: ventromedial PFC, posterior cingulate cortex, bilateral posterior inferior parietal lobe, and bilateral hippocampal formation), and the dorsal attention network (DAN: bilateral middle temporal area MT+, bilateral frontal eye fields and bilateral superior parietal lobes). ROIs were defined in standard MNI space (2 × 2 × 2 mm) as spheres with a 6 mm diameter, centered on peak coordinates based on prior research (Vincent et al. 2008).

Given that coupling of cortical WM areas with striatum is observed during efficient WM functioning (Satterthwaite et al.

2012; Quide et al. 2013), in an additional analysis, striatal ROIs were added to investigate functional connectivity with FPN ROIs. Striatal ROIs were defined as bilateral caudate and putamen in standard space based on the Harvard Oxford Atlas.

For each participant, contrast files for the conditions of interest (1-back, 2-back, 3-back) were then used to extract individual betas (a measure of the BOLD signal's magnitude) in each region of interest (ROIs). The mean values across ROIs belonging to the same network were computed as summary network scores. Group differences in load-dependent up-regulation were then identified with a 3 (network) × 3 (load) × 2 (Group) ANOVA and followed with individual *t*-tests between groups and loads within networks.

To provide supplementary information on load-dependent changes in BOLD response, a voxel-wise general linear model (GLM) was set up for each participant to generate subject-specific contrast (3-back or 2-back vs. 1-back). Subject-specific contrasts were taken into a second level random-effects model using multiple regression. Local maxima with $P < 0.05$ (FDR corrected), and an extent cluster-level threshold of $P < 0.05$ were considered significant. Preprocessing and analyses (both for each subject and for the groups) of the MR data were made using SPM8. Batching was simplified with an in-house developed software, DataZ.

Functional connectivity was computed using in-house MATLAB scripts. Prior to computing functional connectivity estimates, a temporal bandpass filter (0.008–0.1 Hz) was applied to the pre-processed task and resting-state runs and the time-series from a white-matter ROI, a CSF ROI, as well as the motion parameters were removed from the data. Then, functional connectivity was computed for pairwise correlations across all ROIs within a network, and, as a network summary score, we computed mean across all possible pairwise correlations within each network. For the task run, functional connectivity was computed separately for the time points belonging to each condition (1-back, 2-back, 3-back), taking 4-sec BOLD delay into account. Load-dependent differences in functional connectivity analyses were explored using load (3) × group ANOVAs within networks and followed with analyses of individual nodes within a network.

In addition to the motion correction as part of the preprocessing and the consideration of the 6 motion parameters as regressors of no interest in the analyses, the root-mean-square of the 3 translation and 3 rotation parameters was calculated for each volume relative to the preceding volume and averaged across all volumes as a summary measure of motion. The summary measure of head motion will be compared between the two groups to assure that motion differences may not account for differences in brain function.

Genetic Analysis

Blood samples were analyzed for presence of SNPs in genes for the DA D2 receptor (C957T; rs6277), COMT (rs4680), DA- and cAMP-regulated neuronal phosphoprotein (DARPP-32, PPP1R1B; rs879606), and the vesicular monoamine transporter 2 (VMAT2, SLC18A2; rs363387). These SNPs were chosen as they may infer differences in proteins that regulate striatal and frontal DA levels, DA signaling, and vesicular DA storage (Lachman et al. 1996; Hirvonen et al. 2004; Schwab et al. 2005; Kunii et al. 2014), and all have been associated with behavioral differences, including WM performance (Meyer-Lindenberg et al. 2007; Diaz-Asper et al. 2008; Lindenberger et al. 2008; Colzato et al. 2016). Based on previous research, allelic variants were categorized as markers of a beneficial (C-allele of C957T, A-allele of COMT, G-homozygotes for DARPP-32, and G-allele of VMAT2) or less beneficial (T-homozygotes of C957T, G-homozygotes of COMT, A-allele carriers of DARPP-32, and T-homozygotes of VMAT2) DA profile, and scored 1 or 0, respectively. Thus, the summed gene score ranged between 0 and 4. DNA was extracted for the SNPs of interest according to standard procedures. DNA amplification failed for a few reactions, and thus 180 individuals were successfully genotyped for the COMT and C957T SNPs, and 179 for the DARPP-32 and VMAT2 SNPs.

To adjust for multiple comparisons, Bonferroni correction for 6 comparisons for load-dependent BOLD modulation and for functional connectivity during task as well as 11 comparisons for white-matter fractional anisotropy was used. Bonferroni correction for 9 comparisons for offline cognitive measures was used. Finally, effect sizes were computed using Cohen's *d* taking into account unequal sample size and variance.

Results

Behavioral Profiling Reveals Two Performance Subgroups

Latent-profile models specifying between 1 and 5 classes were estimated on the basis of in-scanner WM performance (1-back, 2-back, 3-back). The fit indices are reported in Table 1. The BIC suggested that a model with 3 latent subgroups of equal shape and orientation fitted the data best. The non-significant bootstrapping results for 4 classes ($P = 0.25$) indicated no further improvement when adding one more class. Figure 1A illustrates the 3 latent subgroups in terms of their performance during the n-back task (for clarity, histograms for the different groups are also shown for each task load separately in 1B–D). The figure shows that subgroup 1 ($n = 113$, 63%) is the largest group with relatively higher performance, whereas subgroup 2 ($n = 55$, 31%) displayed lower performance. Subgroup 3 ($n = 12$, 6%) included a few individuals who performed considerably lower than chance level across all 3 n-back conditions (although this group performed well on the offline tasks assessing WM, speed, and episodic memory). It is likely that this group misunderstood the in-scanner task instructions and they were excluded from further analyses, leaving two groups. To further understand the behavioral profile of the two remaining subgroups, they were compared on 3 different cognitive domains tested outside the scanner (WM, episodic memory, and processing speed). A 3 (cognitive domain) × 2 (group) ANOVA revealed a significant task × group interaction for the summary scores of cognitive functions ($F(2332) = 4.16$, $P = 0.02$). Follow-up group comparisons on the cognitive summary score showed that the interaction stemmed from the fact that, whereas subgroup 2 consistently exhibited lower performance relative to subgroup 1, the group difference in offline WM tests ($t(166) = -6.36$, $P < 0.001$; Cohen's $d = 1.47$) was twice as large as for speed ($t(166) = -4.20$,

Table 1 Comparison of Gaussian mixture models on in-scanner N-back data

Solution	*N* params	BIC	LRT	*P*
1 class	9	−3848.84		
2 class	14	−3785.188	89.62	<0.01
3 class	19	−3741.24	69.91	<0.01
4 class	24	−3758.12	9.09	0.28

Params = parameters; BIC = Bayesian information criterion; LRT = Likelihood ratio test.

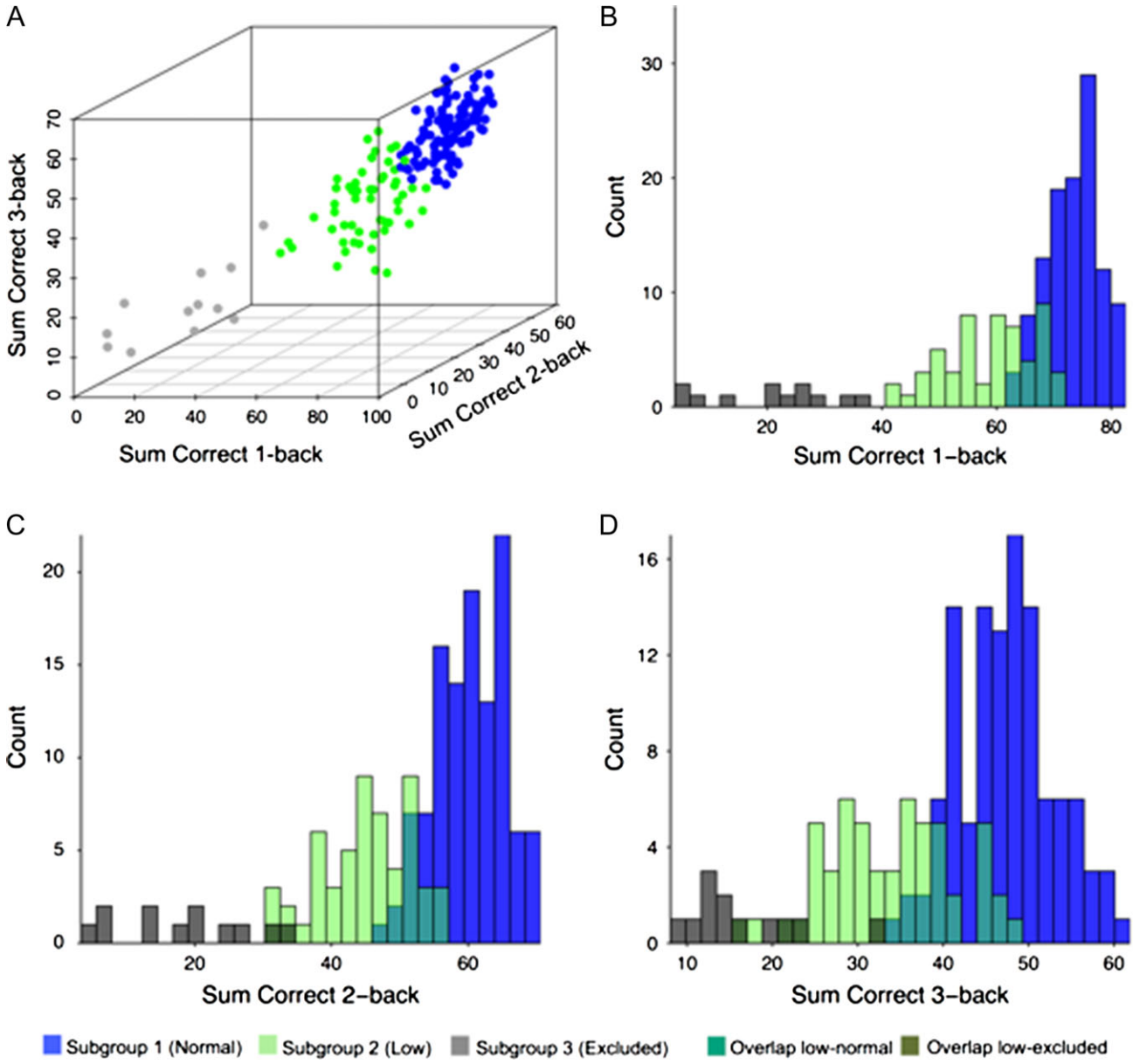

Figure 1. (*A*) Working-memory subgroups identified by latent-class analysis based on in-scanner n-back data for sum correct during 1-back, 2-back and 3-back. (*B–D*) show histograms separated by load.

$P < 0.001$; Cohen's $d = 0.98$) and 3 times as large as for EM ($t(166) = -2.05$, $P < 0.04$; Cohen's $d = 0.49$). Table 2 shows group differences for the individual tasks, and also documents that subgroup 1 outperformed subgroup 2 in a vocabulary test, a measure of crystallized intelligence that was not factored in the summary scores. However, on average, the performance of subgroup 1 on the vocabulary test was not higher than that for an independent reference sample aged 60–66 drawn from a population-based study (cf. Lövdén et al. 2013; Table 1). Similarly, mean accuracy on the in-scanner task for subgroup 1 (1-back 90.5%, 2-back 83.6%, 3-back 75.1%) did not exceed values reported for an independent, age-comparative, sample using n-back in the scanner (cf. Nagel et al. 2011; Fig. 1*B*). Therefore, from here on, we will refer to subgroup 1 as "normal" performers, and to subgroup 2 as "low" performers. No significant differences between the two groups were observed for age, sex (see Supplementary Material for the effect of sex on other brain measures), education, motor ability, work status, or cardiovascular risk factors including nicotine use, high blood pressure, BMI, and medication usage (Supplementary Table 2). Group differences in offline WM summary scores were not accounted for by speed, EM or vocabulary, when those were included as covariates in a linear regression analysis with group as main predictor and WM summary score as outcome ($\beta = 0.32$, $P < 0.001$).

Overall, this suggests that latent profiling of the sample on basis of the in-scanner performance converge with cognitive performance measured outside the scanner, such that the groups were commonly characterized by a pronounced difference in WM. Nevertheless, when latent profiling was run on the 3 offline WM tests instead, a 2-group solution did not overlap perfectly with the in-scanner profiling (Supplementary Table 3). Specifically, 54 out of the 180 subjects received a different group

Table 2 Cognitive performance on the off-line measures for the normal and low-performing groups classified on in-scanner N-back performance

Offline test	Subgroup	Mean	SD	*t*	Cohen's *d*
WM_letter	1 (normal)	35.26	7.20	−3.76*	0.91
	2 (low)	29.98	9.12768		
WM_numerical	1 (normal)	83.71	15.99	−6.31*	1.51
	2 (low)	67.96	13.32		
WM_figural	1 (normal)	14.56	5.45	−3.24*	0.73
	2 (low)	11.44	6.64		
EM_verbal	2 (normal)	13.24	4.16	−1.96	0.46
	2 (low)	11.93	3.88		
EM_numerical	1 (normal)	3.65	2.47	−1.07	0.25
	2 (low)	3.22	2.36		
EM_figural	2 (normal)	12.43	3.79	−1.43	0.34
	2 (low)	11.58	3.13		
PS_verbal	1 (normal)	65.66	15.08	−3.21*	0.75
	2 (low)	57.80	14.60		
PS_numerical	1 (normal)	73.76	15.25	−3.61*	0.85
	2 (low)	64.98	13.85		
PS_figural	1 (normal)	30.35	6.26	−2.49*	0.60
	2 (low)	27.93	5.06		
SRB	1 (normal)	23.65	4.20	−2.96*	0.69
	2 (low)	21.62	4.10		

WM = working memory; PS = processing speed; EM = episodic memory.
*$P < 0.05$.

classification depending on whether profiling was computed on the in-scanner or out-scanner WM data. We therefore report corresponding statistics for all group comparisons also for the 126 individuals who were classified consistently as low or normal in both models in Supplementary Table 4. Finally, because of unequal sample sizes in the two groups, we repeat primary analyses in subsamples matched in sample size in Supplementary Table 4.

Group Differences in Functional Brain Responses

Load-dependent BOLD Response During the n-back fMRI Task

A significant load (3) × network (3) × group (2) interaction shows that group differences in load-dependent BOLD response during n-back differed between networks ($F(4664) = 13.54$, $P < 0.001$). A series of follow-up *t*-tests comparing fMRI signal at each load and in each of the 3 networks between groups showed significant group differences ($P < 0.05$, corrected for multiple comparisons) in FPN (Fig. 2A), but not in DAN or DMN (Supplementary Fig. 1): In FPN, up-regulation in response to increasing task demands was significantly lower for the low-performing subgroup (2-back vs. 1-back: $t(166) = -5.16$, $P < 0.001$; 3-back vs. 1-back: $t(166) = -3.48$, $P < 0.001$; Fig. 2B). Analysis of individual nodes within the FPN revealed that stronger up-regulation from 1-back to 2/3-back in the normal, compared to the low-performing individuals, was pronounced for lateral frontal nodes (Supplementary Fig. 2). These results were further corroborated in a voxel-wise group comparison (Supplementary Fig. 3).

Because groups differed in terms of a measure of crystallized intelligence, the primary analysis was also repeated with SRB score as a covariate. The load (3) × network (3) × group (2) interaction remained significant ($F(4660) = 9.51$, $P < 0.001$).

Across groups, n-back performance (summed across loads) was significantly associated with the magnitude of BOLD up-regulation in FPN nodes from 1-back to 3-back ($r = 0.28$, $P < 0.001$). This association was driven by the normal-performing group (Fig. 2C), demonstrating the usefulness of a data-driven approach to identify latent subgroups rather than relying on behavioral data as a continuous measure.

The reported results largely hold for the conservative subsample excluding 54 subjects, and also for subgroups of normal performers matched in sample size to the low-performing group (Supplementary Tables 4 and 5).

Functional Connectivity of the FPN Nodes During the n-Back fMRI Task and Rest

Because group differences in BOLD up-regulation were predominant for the FPN, we investigated such differences in the functional coupling primarily for this network in a load × group ANOVA. A main effect of load showed that FPN connectivity decreased from 1-back to higher task loads ($F(2332) = 5.81$, $P < 0.01$; $F(2330) = 3.14$, $P = 0.05$ with SRB as covariate; Fig. 3). The correlation matrix of individual task nodes showed that decreases in FPN connectivity were due to a segregation of the network with higher task demands that was driven by an uncoupling of ACC and insular cortex with other nodes in the network (anterior lateral PFC, dlPFC, and lateral parietal cortex, Supplementary Fig. 4). Adding striatal nodes further showed that anterior PFC, dlPFC and lateral parietal cortex, collectively (FPNsub) increased coupling with striatum as a function of load (main effect of load: $F(2330) = 5.86$, $P < 0.01$; $F(2332) = 4.16$, $= 0.02$ with SRB as covariate; Fig. 3B), whereas ACC and insular cortex did not (Supplementary Fig. 4). A main effect of group suggests group differences across loads both for global FPN coupling ($F(1166) = 9.80$, $P = < 0.01$; $F(1165) = 8.18$, $P < 0.01$ with SRB as covariate) and functional connectivity of FPNsub nodes with striatum ($F(1166) = 9.84$, $P < 0.01$; $F(1165) = 10.49$, $P = <0.01$ with SRB as covariate). As shown in Fig. 3, FPN connectivity and FPNsub were lower in the low-performing group than in the normal group. Unlike the load-dependent BOLD response, group differences in FPN connectivity did not vary with increasing task demand for either FPN connectivity (load × group: $F(2330) = 0.71$, $P = 0.50$;, $F(2330) = 1.51$, $P = 0.22$ with SRB as covariate; Fig. 3A) or FPNsub connectivity (load × group: $F(2332) = 0.24$, $P = 0.79$; $F(2330) = 0.06$, $P = 0.94$ with SRB as covariate). This suggests a "trait-like" group difference in terms of network connectivity within FPN and between certain FPN nodes and striatum that is apparent even when the network is taxed very little (i.e., during 1-back). This interpretation was supported by comparing the groups' functional coupling of the FPN during resting state, which also revealed lower connectivity among FPN nodes in the low-performing compared to the normal group (Fig. 3; $t(166) = -2.01$, $P = 0.04$). However, resting-state FPN connectivity was not linked to n-back performance (summed across loads) in either the low group ($r = -0.18$, $P = 0.20$) or the normal group ($r = 0.13$, $P = 0.18$).

Similar to the results on BOLD activation, no significant group difference in functional connectivity was found within DMN at rest ($t(166) = 0.74$, $P = 0.46$) and across different load levels (1-back: $t(166) = -0.47$, $P = 0.64$; 2-back: $t(166) = 0.45$, $P = 0.96$; 3-back: $t(166) = 0.96$, $P = 0.33$). Also, no significant difference for within-network functional connectivity of DAN was found at rest ($t(124) = -0.94$, $P = 0.35$), however tend-level group differences were observed across task load in the DAN, with the low performing subgroups showing trends for lower connectivity among nodes of the DAN than the normal performers during 1-back ($t(166) = -1.78$, $P = 0.08$) and 2-back ($t(166) = -1.81$,

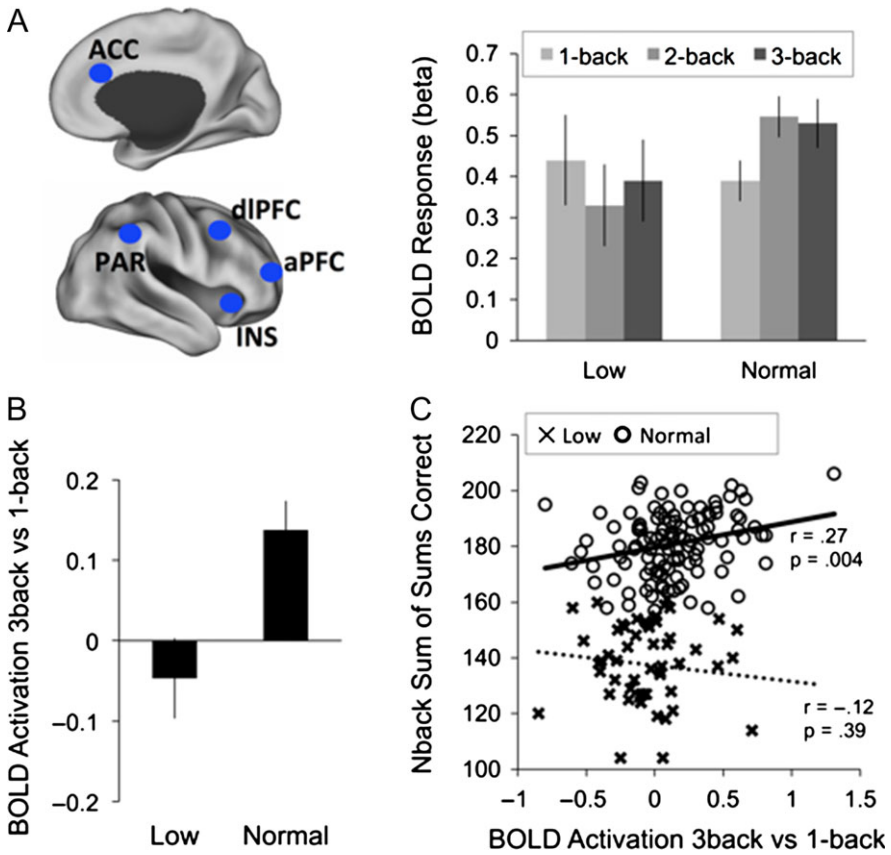

Figure 2. Load-dependent group differences in BOLD response (A) BOLD response (beta) averaged across nodes of the FPN for each group. BOLD response was averaged across a priori selected ROIs in bilateral anterior and dorsolateral PFC (aPFC, dlPFC), anterior cingulate (ACC), bilateral insula (INS), and bilateral inferior parietal lobe (PAR), illustrated here for the right hemisphere. (B) Mean BOLD response up-regulation (3back-1back) by group. (C) Correlation between mean BOLD response up-regulation (3back-1back) and n-back performance (sum of sums for each load) by group. Error bars are standard errors around the means.

$P = 0.07$), and significantly lower connectivity during 3-back ($t(166) = -4.40$, $P < 0.001$).

Functional connectivity data for individual nodes from all networks and for all load conditions are reported in Supplementary Figure 5. They show that group differences across loads are consistently magnified for connections involving the dlPFC and anterior lateral PFC, but these data should be interpreted cautiously because of a lack of control for multiple comparisons.

Summary measures of head motion did not differ between the groups (n-back: $t(166) = 0.93$, $P = 0.36$; rest: $t(166) = 1.45$, $P = 0.15$); thus, the observed differences in FPN and DAN connectivity were not driven by differences in motion. The reported results largely hold for the conservative subsample and also for subgroups of normal performers matched in sample size to that of the low-performing group (Supplementary Tables 4 and 5).

Group Differences in Structural Brain Characteristics

Gray-Matter Volume

We then investigated group differences in gray matter (GM) volume within the FPN. No between-group differences were found when analyzing averaged GM volume across FPN regions ($t(166) = 1.70$; $P > 0.05$), or in corresponding voxel-wise analyses ($P > 0.0001$, uncorrected). Similarly, no group difference in total GM volume was observed ($t(166) = 1.39$; $P > 0.05$), suggesting comparable GM volumes across the two subgroups.

White-Matter Integrity

Next, we probed group differences in white-matter integrity by comparing FA along 11 major white-matter tracts. Similar to the differences in FPN connectivity, the low-performing group exhibited lower FA ($t = 3.2$, $P < 0.005$, Cohen's $d = 0.53$) along the external capsule (Fig. 4, upper panel), when compared to the normal group. By contrast, no significant group differences were observed for FA along the entire skeleton ($t = 1.2$, $P > 0.05$; Fig. 4, upper panel), or along any other major tracts ($Ps > 0.05$).

Cerebral Blood Flow

There were no group differences regarding CBF in the FPN ($Ps > 0.05$ for mean FPN CBF or for CBF of individual FPN ROI seeds). Examining the groups separately, there was a relationship between FPN CBF and an offline WM composite score (i.e., a summary score across 3 WM tasks (Nevalainen et al. 2015)) for the low-performing group ($r = 0.37$, $P < 0.01$), but not for the normal group ($r = -0.10$, $P = 0.33$).

Group Differences in DA D2 Receptor Availability

We found no significant difference in average DA D2 of FPN defined based on the Vincent seed ($P = 0.3$). To further investigate DA D2 differences, we compared whole-brain DA D2 binding potential (BP) values. As compared to the normal group, the

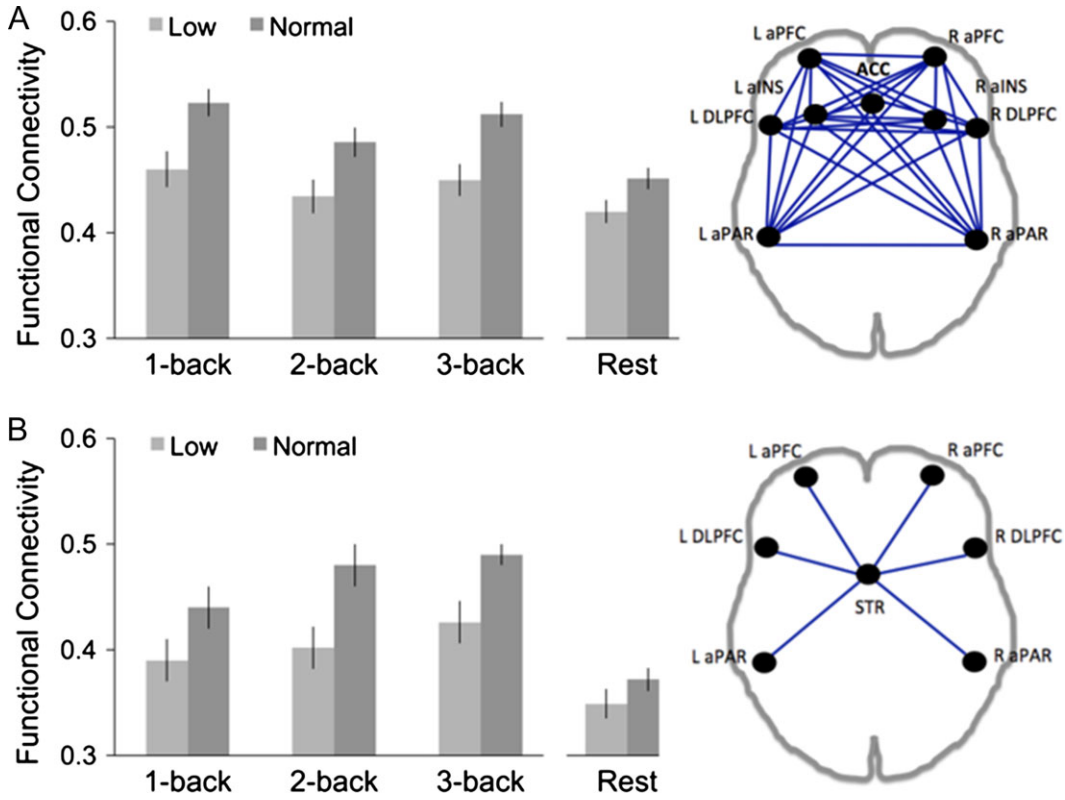

Figure 3. Group differences in functional connectivity of the nodes of the frontal-parietal network during n-back. (*A*) Mean functional connectivity in FPN for each load and rest for each subgroup. Functional connectivity was computed as the average correlation coefficient across all 9 × 9 pairwise correlations in the bilateral anterior and dorsolateral PFC (aPFC, dlPFC), anterior cingulate (ACC), bilateral insula (INS), and bilateral inferior parietal lobe (PAR). (*B*) Mean functional connectivity between select nodes of FPN and striatuam, plotted for each load and rest for each subgroup. Functional connectivity was computed as the mean correlation coefficient of aPFC, dlPFC, and PAR with caudate and putamen (STR). Mean connectivity differences between load conditions for individual nodes are contained in Supplementary Figure 4. Error bars are standard errors around the means.

low-performing group showed lower DA D2 BP in DLPFC (xyz = −26 40 26, t = 3.32, P = 0.0005, k = 45, Cohen's d = 0.62; Fig. 4, lower panel). No group difference in DA D2 BP was observed in striatum even at a liberal threshold ($P > 0.05$). Note also that there was no relationship between CBF and DA D2 in the detected peak (r = 0.01, P = 0.92), suggesting that DA D2 BP difference in dLPFC is unlikely to be driven by local group differences in vascular physiology.

Group Differences in Demographic, Vascular, and Genetic variables

We compared the two subgroups across different demographic variables, cardiovascular risk factors, and for being carriers of beneficial or non-beneficial allelic variants of selected dopaminergic SNPs. No group differences were observed for systolic or diastolic blood pressure or BMI, suggesting that the two groups were comparable on these factors. Furthermore, there were no marked group differences in frequencies of allelic variants of the C957T, COMT, DARPP32, and VMAT2 SNPs, when assessed separately. However, when considering them together as an aggregated gene score, the low-performing group showed a trend of having less beneficial alleles than the normal group (mean score: 1.94 ± 0.81 for low and 2.19 ± 0.77 for normal group; $t(163) = -1.89$, P = 0.06). Interestingly, this trend-level difference turned out to be significant (mean score: 1.88 ± 0.78 for the low and 2.22 ± 0.76 for the normal group; $t(121) = -2.20$, P = 0.030) for the conservative grouping.

The reported results for white matter integrity, perfusion, DA largely hold for the conservative grouping that excluded 54 subjects (Supplementary Table 4).

Discussion

The primary goal of this study was to examine individual differences in WM performance and their brain correlates in a large age-homogenous cohort of healthy adults in their mid-60s, a time at which cognitive decline typically begins (Rönnlund et al. 2005; Gorbach et al. 2016).

Using LPA on in-scanner n-back performance, two dominant subgroups were identified. One of these included a large group of individuals that performed around the sample mean, whereas the other group performed at a lower level. Past work indicates substantial inter-individual differences in WM performance for both younger (Nagel et al. 2009, 2011) and older (Nyberg et al. 2013) adults, but with relatively large age bins within each group (e.g., 20–40 years-old in the younger group; 60–80 years-old in older group). Our findings extend previous reports by demonstrating considerable inter-individual variability in WM performance also within a narrow age bin of older adults.

Individual differences in WM performance have been linked to differences in activation and connectivity within the FPN (Osaka et al. 2003, 2004; Vogel et al. 2005; Nagel et al. 2009, 2011). Our results for BOLD responsivity within the canonical FPN WM revealed that the degree of load-dependent modulation in the FPN was greater in the normal compared to the low-performing

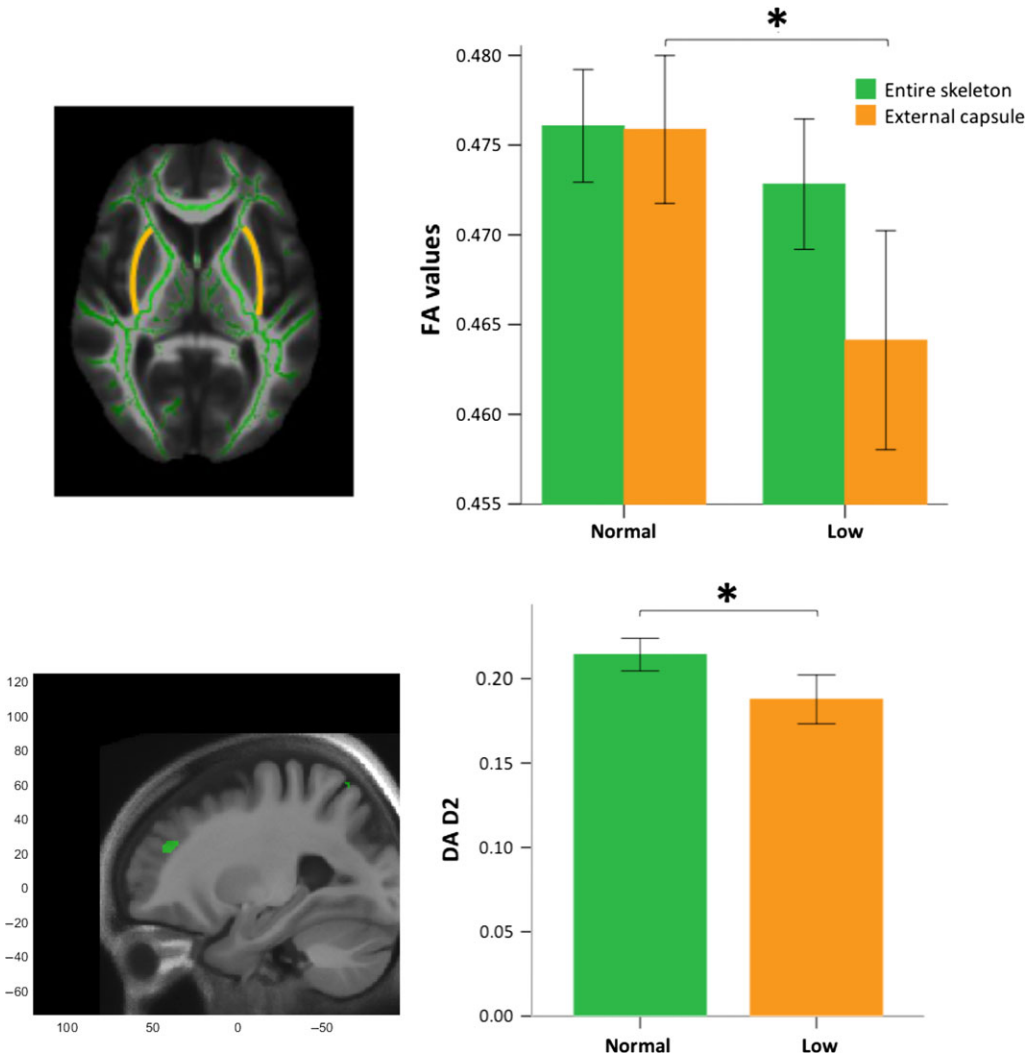

Figure 4. Group differences in white-matter integrity (upper panel) and DA D2 BP in frontal cortex (lower panel) *$P < 0.005$. Error bars are standard errors around the means.

subgroup. Moreover, both the ROI and voxel-wise analyses yielded a neural correlate of group by WM load in FPN, particularly for the DLPFC. The combined observations that resting FPN CBF, and WM performance were coupled in the low-performing group, and that this group failed to express a load-dependent vascular response support the view that resting blood flow becomes more indicative of the amount of neural resources that can be assigned to a task when the maximum capacity is reached. The observed difference in FPN response may reflect not only differences in the amount of storage space, but also individual differences in consistently deploying attentional control over what is stored in WM (Adam et al. 2015). On this view, the low-performing subgroup might have more difficulty ignoring distracting information (Fukuda and Vogel 2011; Eriksson et al. 2015).

Results from functional connectivity analyses during n-back revealed lower connectivity within the FPN and DAN in the low-performing compared to the normal group across all load levels. A similar group difference in resting-state connectivity was observed for FPN, but not for DAN, suggesting state-invariant and state-dependent differences in FPN and DAN between groups, respectively. This finding adds to an emerging literature that task-free fMRI can only uncover parts of the relevant individual differences in brain function (Geerligs et al. 2015; Avelar-Pereira et al. 2017; Campbell and Schacter 2017). The trait-like nature of FPN connectivity is also in agreement with reports of stable inter-individual differences in WM over time (Kane and Engle 2002). A trend for decreases in FPN connectivity at higher cognitive loads (2-back and 3-back) compared with the lower cognitive load (1-back) (Fig. 3B) was found in both subgroups. This finding is in line with a previous study, which reported a similar trend for FPN modularity (Liang et al. 2016). Here, we provide new evidence that decreases in FPN connectivity with increasing load reflect a segregation of the FPN network nodes, such that DLPFC, lateral anterior PFC, and lateral parietal areas increase coupling with striatum with increased task loads, whereas insula and ACC do not. These patterns of network segregation with increased task demands would not be revealed in voxel-wise analyses (e.g., Nagel et al. 2009), which selectively look only for the increases common to a set of nodes.

In line with the idea that resting-state functional connectivity may, to some extent, reflect underlying structural connectivity (Damoiseaux and Greicius 2009; Greicius et al. 2009), our

structural connectivity analyses revealed a selective group difference along the external capsule, with the low-performing subgroup showing lower white-matter integrity. The external capsule is part of a dense bundle connecting the prefrontal, parietal, and temporal cortex (Charlton et al. 2010). Critically, the integrity of this tract is a strong correlate of WM performance (Charlton et al. 2010). Note that our DTI analysis was exploratory and we found no group difference elsewhere. It is noteworthy that while using conservative grouping, we additionally found a group-difference along the left superior longitudinal fasciculus (Supplementary Table 4) which is strongly linked to the FPN circuit (Ostby et al. 2011). Our connectivity analyses suggest that lower white-matter integrity in one of the tracts which is linked to fronto-parietal circuit might be linked to lower functional coupling among key WM regions, which is reflected in less efficient up-regulation of activity during the task and lower WM performance. Latent profiling further suggested that around 30% of older adults show this specific deficit, which prompted us to investigate possible neurobiological markers that could further characterize this group.

Utilizing information from a PET scan, we discovered lower DA D2 availability in the DLPFC region of the FPN in the low-performing compared to the normal group. These results are in line with pharmacological work suggesting that D2 receptor agonists and antagonists might affect different aspects of WM performance (Mehta et al. 2004; van Holstein et al. 2011). Note that, although extrastriatal D2DR availability has been detected with [^{11}C] raclopride (Garraux et al. 2007; Sawamoto et al. 2008), and with high test–retest reliability (Alakurtti et al. 2015), this low-affinity ligand is not ideal for imaging of extrastriatal D2 receptors. However, the reported DA D2 binding values for the DLPFC were in the expected range (10% of caudate levels (Hall et al. 1994)). The signal was positive and significantly higher compared with the receptor-free cerebellar region and without any confounding relationship to regional CBF. Our results of lower DA D2 receptor availability in DLPFC in the low-performing subgroup with lower fronto-parietal integrity, along with a trend toward a less beneficial DA gene profile, extend previous results of lower frontal efficiency in individuals with genetic predispositions for lower synaptic DA levels in prefrontal cortex (Nyberg et al. 2013). Whereas inferences on DA system integrity were based on individual differences in COMT val/met allele composition only in Nyberg et al. (2013), here DA receptor availability was directly measured using PET. Notably, the contribution of the PET-derived measure of D2 receptor availability to WM is likely due to the modulatory effects of D2 receptors on updating processes (for review, see D'Esposito and Postle 2015). By contrast, animal data suggest that maintenance of representations in WM is more related to the D1 receptor system (Sawaguchi, 2001; Wang, Vijayraghavan and Goldman-Rakic, 2004). Finally, our group difference in DA D2 of DLPFC should be interpreted with caution, given the nature of the voxel-wise analysis of binding potential, which might be affected by some confounding factors such as signal drop out.

Results of individual differences in in-scanner WM performance mapped well with differences in the offline cognitive measure. The low-performing group performed worse than the normal group on all WM and processing speed tasks, although the groups performed quite comparable on the episodic memory tasks. The fact that the two groups showed similar differences on the WM and speed tasks is consistent with the notion that the speed with which adequate internal representations can be established is a critical factor for WM functioning (Salthouse 1994; Ackerman et al. 2002; Colom 2004). Similarly, despite lower structural and functional connectivity within the FPN and lower DA D2 receptor availability in the DLPFC, the low-performing subgroup were comparable to the normal group in brain measures relevant for episodic memory (i.e., DMN structural and functional connectivity, and hippocampal volume). These findings suggest that the low-performing individuals have a specific WM impairment, but a relatively intact episodic memory system. That said, it should be noted that the n-back task is complex and taxes many processes, such as response inhibition. Thus, the group difference in WM might be partly influenced by a difference in response inhibition. Although LPA was a fairly successful approach to identify different WM subgroups based on n-back data, an alternative model based on the 3 WM offline tests only partially overlapped with the initial model (Supplementary Table 4). This suggests that some aspects of the n-back data might be different from the offline WM tests.

In conclusion, our findings provide novel and converging evidence for the existence of a subgroup of older adults with impaired WM functioning characterized by reduced cortico-cortical communication and altered neurochemical signatures within the FPN.

Supplementary Material

Supplementary material is available at *Cerebral Cortex* online.

Funding

This work was funded by the Swedish Research Council, Umeå Universitet, Umeå University–Karolinska Institute Strategic Neuroscience Program, the Knut and Alice Wallenberg Foundation, the Torsten and Ragnar Söderberg Foundation, an Alexander von Humboldt Research award, a donation from the Jochnick Foundation, Swedish Brain Power, Swedish Brain Foundation, Västerbotten County Council, Innovation Fund of the Max Planck Society, and the 2010 Gottfried Wilhelm Leibniz Research Award.

References

Ackerman PL, Beier ME, Boyle MD. 2002. Individual differences in working memory within a nomological network of cognitive and perceptual speed abilities. J Exp Psychol Gen. 131: 567–589.

Adam KC, Mance I, Fukuda K, Vogel EK. 2015. The contribution of attentional lapses to individual differences in visual working memory capacity. J Cogn Neurosci. 27:1601–1616.

Alakurtti K, Johansson JJ, Joutsa J, Laine M, Backman L, Nyberg L, Rinne JO. 2015. Long-term test-retest reliability of striatal and extrastriatal dopamine D2/3 receptor binding: study with [(11)C]raclopride and high-resolution PET. J Cereb Blood Flow Metab. 35:1199–1205.

Ashburner J. 2007. A fast diffeomorphic image registration algorithm. NeuroImage. 38:95–113.

Ashburner J, Friston KJ. 2005. Unified segmentation. NeuroImage. 26:839–851.

Avelar-Pereira B, Bäckman L, Wåhlin A, Nyberg L, Salami A. 2017. Age-related differences in dynamic interactions among default mode, frontoparietal control, and dorsal attention networks during resting-state and interference resolution. Front Aging Neurosci. 9:152.

Barnes JJ, Dean AJ, Nandam LS, O'Connell RG, Bellgrove MA. 2011. The molecular genetics of executive function: role of monoamine system genes. Biol Psychiatry. 69:e127–e143.

Boone KB. 1999. Neuropsychological assessment of executive functions: impact of age, education, gender, intellectual level, and vascular status on executive test scores. In: MillerBL, CummingsJL, editors. The human frontal lobes: functions and disorders. The science and practice of neuropsychology series. New York: Guilford Press. p. 247–260.

Buckner RL. 2004. Memory and executive function in aging and AD: multiple factors that cause decline and reserve factors that compensate. Neuron. 44:195–208.

Burzynska AZ, Nagel IE, Preuschhof C, Gluth S, Backman L, Li SC, Lindenberger U, Heekeren HR. 2012. Cortical thickness is linked to executive functioning in adulthood and aging. Hum Brain Mapp. 33:1607–1620.

Burzynska AZ, Nagel IE, Preuschhof C, Li SC, Lindenberger U, Backman L, Heekeren HR. 2011. Microstructure of frontoparietal connections predicts cortical responsivity and working memory performance. Cereb Cortex. 21:2261–2271.

Bäckman L, Lindenberger U, Li SC, Nyberg L. 2010. Linking cognitive aging to alterations in dopamine neurotransmitter functioning: recent data and future avenues. Neurosci Biobehav Rev. 34:670–677.

Bäckman L, Nyberg L, Soveri A, Johansson J, Andersson M, Dahlin E, Neely AS, Virta J, Laine M, Rinne JO. 2011. Effects of working-memory training on striatal dopamine release. Science. 333:718.

Cabeza R, Nyberg L, Park DC. 2016. Cognitive neuroscience of aging: linking cognitive and cerebral aging. NY: Oxford University Press.

Campbell KL, Schacter DL. 2017. Aging and the resting state: cognition is not obsolete. Lang Cogn Neurosci. 32:692–694.

Charlton RA, Barrick TR, Lawes IN, Markus HS, Morris RG. 2010. White matter pathways associated with working memory in normal aging. Cortex. 46:474–489.

Colom R. 2004. Working memory is (almost) perfectly predicted by g. Intelligence. 32:277–296.

Colzato LS, Steenbergen L, Sellaro R, Stock AK, Arning L, Beste C. 2016. Effects of l-Tyrosine on working memory and inhibitory control are determined by DRD2 genotypes: a randomized controlled trial. Cortex. 82:217–224.

Cools R, D'Esposito M. 2011. Inverted-U-shaped dopamine actions on human working memory and cognitive control. Biol Psychiatry. 69:e113–e125.

Dahlin E, Neely AS, Larsson A, Backman L, Nyberg L. 2008. Transfer of learning after updating training mediated by the striatum. Science. 320:1510–1512.

Damoiseaux JS, Greicius MD. 2009. Greater than the sum of its parts: a review of studies combining structural connectivity and resting-state functional connectivity. Brain Struct Funct. 213:525–533.

Darki F, Klingberg T. 2015. The role of fronto-parietal and fronto-striatal networks in the development of working memory: a longitudinal study. Cereb Cortex. 25:1587–1595.

Davis SW, Dennis NA, Buchler NG, White LE, Madden DJ, Cabeza R. 2009. Assessing the effects of age on long white matter tracts using diffusion tensor tractography. NeuroImage. 46:530–541.

Devanand DP, Pradhaban G, Liu X, Khandji A, De Santi S, Segal S, Rusinek H, Pelton GH, Honig LS, Mayeux R, et al. 2007. Hippocampal and entorhinal atrophy in mild cognitive impairment: prediction of Alzheimer disease. Neurology. 68: 828–836.

Di X, Rypma B, Biswal BB. 2014. Correspondence of executive function related functional and anatomical alterations in aging brain. Prog Neuro-Psychopharmacol Biol Psychiatry. 48:41–50.

Diaz-Asper CM, Goldberg TE, Kolachana BS, Straub RE, Egan MF, Weinberger DR. 2008. Genetic variation in catechol-O-methyltransferase: effects on working memory in schizophrenic patients, their siblings, and healthy controls. Biol Psychiatry. 63:72–79.

Dureman I 1960. SRB: 1. Stockholm, Sweden: Psykologiforlaget.

D'Esposito M, Postle BR. 2015. The cognitive neuroscience of working memory. Annu Rev Psychol. 66:115–142.

Eriksson J, Vogel EK, Lansner A, Bergstrom F, Nyberg L. 2015. Neurocognitive architecture of working memory. Neuron. 88:33–46.

Fandako Y, Shing YL, Lindenberger U. 2012. Heterogeneity in memory training improvement among older adults: a latent class analysis. Memory. 20:554–567.

Flensborg Damholdt M, Shevlin M, Borghammer P, Larsen L, Ostergaard K. 2012. Clinical heterogeneity in Parkinson's disease revisited: a latent profile analysis. Acta Neurol Scand. 125:311–318.

Floresco SB, Magyar O, Ghods-Sharifi S, Vexelman C, Tse MT. 2006. Multiple dopamine receptor subtypes in the medial prefrontal cortex of the rat regulate set-shifting. Neuropsychopharmacology. 31:297–309.

Frank MJ, Loughry B, O'Reilly RC. 2001. Interactions between frontal cortex and basal ganglia in working memory: a computational model. Cogn Affect Behav Neurosci. 1:137–160.

Fukuda K, Vogel EK. 2011. Individual differences in recovery time from attentional capture. Psychol Sci. 22:361–368.

Garraux G, Peigneux P, Carson RE, Hallett M. 2007. Task-related interaction between basal ganglia and cortical dopamine release. J Neurosci. 27:14434–14441.

Geerligs L, Rubinov M, Cam C, Henson RN. 2015. State and trait components of functional connectivity: individual differences vary with mental state. J Neurosci. 35:13949–13961.

Glisky EL, Rubin SR, Davidson PS. 2001. Source memory in older adults: an encoding or retrieval problem? J Exp Psychol. 27: 1131–1146.

Gorbach T, Pudas S, Lundquist A, Oradd G, Josefsson M, Salami A, de Luna X, Nyberg L. 2016. Longitudinal association between hippocampus atrophy and episodic-memory decline. Neurobiol Aging. 51:167–176.

Grady C, Sarraf S, Saverino C, Campbell K. 2016. Age differences in the functional interactions among the default, frontoparietal control, and dorsal attention networks. Neurobiol Aging. 41:159–172.

Greicius MD, Supekar K, Menon V, Dougherty RF. 2009. Resting-state functional connectivity reflects structural connectivity in the default mode network. Cereb Cortex. 19:72–78.

Gunning-Dixon FM, Raz N. 2003. Neuroanatomical correlates of selected executive functions in middle-aged and older adults: a prospective MRI study. Neuropsychologia. 41:1929–1941.

Hall H, Sedvall G, Magnusson O, Kopp J, Halldin C, Farde L. 1994. Distribution of D1- and D2-dopamine receptors, and dopamine and its metabolites in the human brain. Neuropsychopharmacology. 11:245–256.

Hayden KM, Reed BR, Manly JJ, Tommet D, Pietrzak RH, Chelune GJ, Yang FM, Revell AJ, Bennett DA, Jones RN. 2011. Cognitive decline in the elderly: an analysis of population heterogeneity. Age Ageing. 40:684–689.

Hirvonen M, Laakso A, Nagren K, Rinne JO, Pohjalainen T, Hietala J. 2004. C957T polymorphism of the dopamine D2 receptor (DRD2) gene affects striatal DRD2 availability in vivo. Mol Psychiatry. 9:1060–1061.

Hirvonen MM, Laakso A, Nagren K, Rinne JO, Pohjalainen T, Hietala J. 2009. C957T polymorphism of dopamine D2

receptor gene affects striatal DRD2 in vivo availability by changing the receptor affinity. Synapse. 63:907–912.

Huang AS, Klein DN, Leung HC. 2016. Load-related brain activation predicts spatial working memory performance in youth aged 9-12 and is associated with executive function at earlier ages. Dev Cogn Neurosci. 17:1–9.

Jockwitz C, Caspers S, Lux S, Eickhoff SB, Jütten K, Lenzen S, Moebus S, Pundt N, Reid A, Hoffstaedter F, et al. 2017. Influence of age and cognitive performance on resting-state brain networks of older adults in a population-based cohort. Cortex. 89:28–44.

Josefsson M, de Luna X, Pudas S, Nilsson LG, Nyberg L. 2012. Genetic and lifestyle predictors of 15-year longitudinal change in episodic memory. J Am Geriatr Soc. 60:2308–2312.

Kane MJ, Engle RW. 2002. The role of prefrontal cortex in workingmemory capacity, executive attention, and general fluid intelligence: an individual-differences perspective. Psychol Bull Rev. 9:637–671.

Kantarci K, Lesnick T, Ferman TJ, Przybelski SA, Boeve BF, Smith GE, Kremers WK, Knopman DS, Jack CR Jr., Petersen RC. 2016. Hippocampal volumes predict risk of dementia with Lewy bodies in mild cognitive impairment. Neurology. 87:2317–2323.

Ko KJ, Berg CA, Butner J, Uchino BN, Smith TW. 2007. Profiles of successful aging in middle-aged and older adult married couples. Psychol Aging. 22:705–718.

Kunii Y, Hyde TM, Ye T, Li C, Kolachana B, Dickinson D, Weinberger DR, Kleinman JE, Lipska BK. 2014. Revisiting DARPP-32 in postmortem human brain: changes in schizophrenia and bipolar disorder and genetic associations with t-DARPP-32 expression. Mol Psychiatry. 19:192–199.

Lachman HM, Papolos DF, Saito T, Yu YM, Szumlanski CL, Weinshilboum RM. 1996. Human catechol-O-methyltransferase pharmacogenetics: description of a functional polymorphism and its potential application to neuropsychiatric disorders. Pharmacogenetics. 6:243–250.

Leemans A, Jones DK. 2009. The B-matrix must be rotated when correcting for subject motion in DTI data. Magn Reson Med. 61:1336–1349.

Li SC, Papenberg G, Nagel IE, Preuschhof C, Schroder J, Nietfeld W, Bertram L, Heekeren HR, Lindenberger U, Backman L. 2013. Aging magnifies the effects of dopamine transporter and D2 receptor genes on backward serial memory. Neurobiol Aging. 34:358 e1–e10.

Liang X, Zou Q, He Y, Yang Y. 2016. Topologically reorganized connectivity architecture of default-mode, executive-control, and salience networks across working memory task loads. Cereb Cortex. 26:1501–1511.

Lindenberger U. 2014. Human cognitive aging: corriger la fortune? Science. 346:572–578.

Lindenberger U, Nagel IE, Chicherio C, Li SC, Heekeren HR, Backman L. 2008. Age-related decline in brain resources modulates genetic effects on cognitive functioning. Front Neurosci. 2:234–244.

Logan J, Fowler JS, Volkow ND, Wolf AP, Dewey SL, Schlyer DJ, MacGregor RR, Hitzemann R, Bendriem B, Gatley SJ, et al. 1990. Graphical analysis of reversible radioligand binding from time-activity measurements applied to [N-11C-methyl]-(-)-cocaine PET studies in human subjects. J Cereb Blood Flow Metab. 10:740–747.

Lövden M, Karalija N, Andersson M, Wåhlin A, Axelsson J, Köhncke Y, Jonasson LS, Rieckmann A, Papenberg G, Garrett D, et al. 2017. Latent-profile analysis reveals behavioral and brain correlates of dopamine-cognition associations. Cereb Cortex. 1–14.

Lövden M, Laukka EJ, Rieckmann A, Kalpouzos G, Li TQ, Jonsson T, Wahlund LO, Fratiglioni L, Backman L. 2013. The dimensionality of between-person differences in white matter microstructure in old age. Hum Brain Mapp. 34: 1386–1398.

Mak E, Su L, Williams GB, Watson R, Firbank M, Blamire A, O'Brien J. 2016. Differential atrophy of hippocampal subfields: a comparative study of dementia with Lewy bodies and Alzheimer disease. Am J Geriatr Psychiatry. 24:136–143.

Manard M, Bahri MA, Salmon E, Collette F. 2016. Relationship between grey matter integrity and executive abilities in aging. Brain Res. 1642:562–580.

Mehta MA, Manes FF, Magnolfi G, Sahakian BJ, Robbins TW. 2004. Impaired set-shifting and dissociable effects on tests of spatial working memory following the dopamine D2 receptor antagonist sulpiride in human volunteers. Psychopharmacology. 176:331–342.

Meyer-Lindenberg A, Straub RE, Lipska BK, Verchinski BA, Goldberg T, Callicott JH, Egan MF, Huffaker SS, Mattay VS, Kolachana B, et al. 2007. Genetic evidence implicating DARPP-32 in human frontostriatal structure, function, and cognition. J Clin Invest. 117:672–682.

Nagel IE, Chicherio C, Li SC, von Oertzen T, Sander T, Villringer A, Heekeren HR, Backman L, Lindenberger U. 2008. Human aging magnifies genetic effects on executive functioning and working memory. Front Hum Neurosci. 2:1.

Nagel IE, Preuschhof C, Li SC, Nyberg L, Backman L, Lindenberger U, Heekeren HR. 2009. Performance level modulates adult age differences in brain activation during spatial working memory. Proc Natl Acad Sci U S A. 106: 22552–22557.

Nagel IE, Preuschhof C, Li SC, Nyberg L, Backman L, Lindenberger U, Heekeren HR. 2011. Load modulation of BOLD response and connectivity predicts working memory performance in younger and older adults. J Cogn Neurosci. 23:2030–2045.

Nevalainen N, Riklund K, Andersson M, Axelsson J, Ogren M, Lovden M, Lindenberger U, Backman L, Nyberg L. 2015. COBRA: a prospective multimodal imaging study of dopamine, brain structure and function, and cognition. Brain Res. 1612:83–103.

Newton AT, Morgan VL, Rogers BP, Gore JC. 2011. Modulation of steady state functional connectivity in the default mode and working memory networks by cognitive load. Hum Brain Mapp. 32:1649–1659.

Nikolova YS, Ferrell RE, Manuck SB, Hariri AR. 2011. Multilocus genetic profile for dopamine signaling predicts ventral striatum reactivity. Neuropsychopharmacology. 36:1940–1947.

Nyberg L, Andersson M, Kauppi K, Lundquist A, Persson J, Pudas S, Nilsson LG. 2013. Age-related and genetic modulation of frontal cortex efficiency. J Cogn Neurosci. 26:746–754.

Nyberg L, Bäckman L. 2010. Memory changes and the aging brain: a multimodal imaging approach. In: SvhairKW, WillisSL, editors. Handbook of the psychology of aging. London, United Kingdom: Academic Press. p. 121–132.

Nyberg L, Dahlin E, Stigsdotter Neely A, Backman L. 2009. Neural correlates of variable working memory load across adult age and skill: dissociative patterns within the frontoparietal network. Scand J Psychol. 50:41–46.

Nyberg L, Karalija N, Salami A, Andersson M, Wåhlin A, Kaboodvand N, Köhncke Y, Axelsson J, Rieckmann A, Papenberg G, et al. 2016. Dopamine D2 receptor availability is linked to hippocampal–caudate functional connectivity and episodic memory. Proc Natl Acad Sci USA. 113:7918–7923.

Nyberg L, Lovden M, Riklund K, Lindenberger U, Backman L. 2012. Memory aging and brain maintenance. Trends Cogn Sci. 16: 292–305.

Osaka M, Osaka N, Kondo H, Morishita M, Fukuyama H, Aso T, Shibasaki H. 2003. The neural basis of individual differences in working memory capacity: an fMRI study. NeuroImage. 18: 789–797.

Osaka N, Osaka M, Kondo H, Morishita M, Fukuyama H, Shibasaki H. 2004. The neural basis of executive function in working memory: an fMRI study based on individual differences. NeuroImage. 21:623–631.

Ostby Y, Tamnes CK, Fjell AM, Walhovd KB. 2011. Morphometry and connectivity of the fronto-parietal verbal working memory network in development. Neuropsychologia. 49: 3854–3862.

Ott T, Nieder A. 2016. Dopamine D2 receptors enhance population dynamics in primate prefrontal working memory circuits. Cereb Cortex. 27:4423–4435.

Papenberg G, Salami A, Persson J, Lindenberger U, Backman L. 2015. Genetics and functional imaging: effects of APOE, BDNF, COMT, and KIBRA in aging. Neuropsychol Rev. 25:47–62.

Plumet J, Gil R, Gaonach D. 2005. Neuropsychological assessment of executive functions in women: effects of age and education. Neuropsychology. 19:566–577.

Pruchno RA, Wilson-Genderson M, Rose M, Cartwright F. 2010. Successful aging: early influences and contemporary characteristics. Gerontologist. 50:821–833.

Puig MV, Miller EK. 2015. Neural substrates of dopamine D2 receptor modulated executive functions in the monkey prefrontal cortex. Cereb Cortex. 25:2980–2987.

Quide Y, Morris RW, Shepherd AM, Rowland JE, Green MJ. 2013. Task-related fronto-striatal functional connectivity during working memory performance in schizophrenia. Schizophr Res. 150:468–475.

Raz N, Gunning FM, Head D, Dupuis JH, McQuain J, Briggs SD, Loken WJ, Thornton AE, Acker JD. 1997. Selective aging of the human cerebral cortex observed in vivo: differential vulnerability of the prefrontal gray matter. Cereb Cortex. 7:268–282.

Rieckmann A, Karlsson S, Karlsson P, Brehmer Y, Fischer H, Farde L, Nyberg L, Backman L. 2011. Dopamine D1 receptor associations within and between dopaminergic pathways in younger and elderly adults: links to cognitive performance. Cereb Cortex. 21:2023–2032.

Rönnlund M, Nyberg L, Backman L, Nilsson LG. 2005. Stability, growth, and decline in adult life span development of declarative memory: cross-sectional and longitudinal data from a population-based study. Psychol Aging. 20:3–18.

Salami A, Eriksson J, Nilsson LG, Nyberg L. 2011. Age-related white matter microstructural differences partly mediate age-related decline in processing speed but not cognition. Biochim Biophys Acta. 1822:408–415.

Salami A, Pudas S, Nyberg L. 2014. Elevated hippocampal resting-state connectivity underlies deficient neurocognitive function in aging. Proc Natl Acad Sci U S A. 111:17654–17659.

Salami A, Rieckmann A, Fischer H, Backman L. 2013. A multivariate analysis of age-related differences in functional networks supporting conflict resolution. NeuroImage. 86:150–163.

Salthouse T. 1994. The aging of working memory. Neuropsychology. 8:535–543.

Satterthwaite TD, Ruparel K, Loughead J, Elliott MA, Gerraty RT, Calkins ME, Hakonarson H, Gur RC, Gur RE, Wolf DH. 2012. Being right is its own reward: load and performance related ventral striatum activation to correct responses during a working memory task in youth. NeuroImage. 61:723–729.

Sawamoto N, Piccini P, Hotton G, Pavese N, Thielemans K, Brooks DJ. 2008. Cognitive deficits and striato-frontal dopamine release in Parkinson's disease. Brain. 131:1294–1302.

Scheltens NM, Galindo-Garre F, Pijnenburg YA, van der Vlies AE, Smits LL, Koene T, Teunissen CE, Barkhof F, Wattjes MP, Scheltens P, et al. 2016. The identification of cognitive subtypes in Alzheimer's disease dementia using latent class analysis. J Neurol Neurosurg Psychiatry. 87:235–243.

Schwab SG, Franke PE, Hoefgen B, Guttenthaler V, Lichtermann D, Trixler M, Knapp M, Maier W, Wildenauer DB. 2005. Association of DNA polymorphisms in the synaptic vesicular amine transporter gene (SLC18A2) with alcohol and nicotine dependence. Neuropsychopharmacology. 30:2263–2268.

Smith SM. 2002. Fast robust automated brain extraction. Hum Brain Mapp. 17:143–155.

Spencer-Smith M, Ritter BC, Murner-Lavanchy I, El-Koussy M, Steinlin M, Everts R. 2013. Age, sex, and performance influence the visuospatial working memory network in childhood. Dev Neuropsychol. 38:236–255.

Sawaguchi T. 2001. The effects of dopamine and its antagonists on directional delay-period activity of prefrontal neurons in monkeys during an oculomotor delayed-response task. Neurosci Res. 41:115–128.

Takeuchi H, Taki Y, Nouchi R, Hashizume H, Sekiguchi A, Kotozaki Y, Nakagawa S, Miyauchi CM, Sassa Y, Kawashima R. 2013. Effects of working memory training on functional connectivity and cerebral blood flow during rest. Cortex. 49: 2106–2125.

van Holstein M, Aarts E, van der Schaaf ME, Geurts DE, Verkes RJ, Franke B, van Schouwenburg MR, Cools R. 2011. Human cognitive flexibility depends on dopamine D2 receptor signaling. Psychopharmacology. 218:567–578.

Vermunt J, Magidson J. 2002. Latent class cluster analysis. Cambridge University Press. p. 89–106.

Vernooij MW, Wielopolski PA, Niessen WJ. 2009. White matter microstructural integrity and cognitive function in a general elderly population. Arch Gen Psychiatry. 66:545–553.

Vincent JL, Kahn I, Snyder AZ, Raichle ME, Buckner RL. 2008. Evidence for a frontoparietal control system revealed by intrinsic functional connectivity. J Neurophysiol. 100: 3328–3342.

Vogel EK, McCollough AW, Machizawa MG. 2005. Neural measures reveal individual differences in controlling access to working memory. Nature. 438:500–503.

Volkow ND, Wang GJ, Fowler JS, Logan J, Gatley SJ, MacGregor RR, Schlyer DJ, Hitzemann R, Wolf AP. 1996. Measuring age-related changes in dopamine D2 receptors with 11C-raclopride and 18F-N-methylspiroperidol. Psychiatry Res. 67: 11–16.

Wakana S, Jiang Y, Nagae-Poetscher L, Van Zijl PCM, Mori S. 2004. Fiber tract–based atlas of human white matter anatomy. Radiology. 230:77–87.

Wallsten E, Axelsson J, Sundstrom T, Riklund K, Larsson A. 2013. Subcentimeter tumor lesion delineation for high-resolution 18F-FDG PET images: optimizing correction for partial-volume effects. J Nucl Med Technol. 41:85–91.

Wang M, Vijayraghavan S, Goldman-Rakic PS. 2004. Selective D2 receptor actions on the functional circuitry of working memory. Science. 303:853–856.

West RL. 1996. An application of prefrontal cortex function theory to cognitive aging. Psychol Bull. 120:272–292.

Yuan P, Raz N. 2014. Prefrontal cortex and executive functions in healthy adults: a meta-analysis of structural neuroimaging studies. Neurosci Biobehav Rev. 42:180–192.